Retinal Photoreceptors of Two Subterranean Tuco-tuco Species (Rodentia, *Ctenomys*): Morphology, Topography, and Spectral Sensitivity

Cristian E. Schleich,[1]* Alex Vielma,[2] Martin Glösmann,[3] Adrian G. Palacios,[2] and Leo Peichl[4]

[1]Laboratorio Ecofisiología, Facultad de Ciencias Exactas y Naturales, Universidad Nacional de Mar del Plata, Argentina; Conicet
[2]Centro de Neurociencia de Valparaíso, Facultad de Ciencias, Universidad de Valparaíso, Chile
[3]Institute of Physiology and Pathophysiology, University of Veterinary Medicine Vienna, Vienna, Austria
[4]Max Planck Institute for Brain Research, Frankfurt am Main, Germany

ABSTRACT

Traditionally, vision was thought to be useless for animals living in dark underground habitats, but recent studies in a range of subterranean rodent species have shown a large diversity of eye features, from small subcutaneous eyes to normal-sized functional eyes. We analyzed the retinal photoreceptors in the subterranean hystricomorph rodents *Ctenomys talarum* and *Ctenomys magellanicus* to elucidate whether adaptation was to their near-lightless burrows or rather to their occasional diurnal surface activity. Both species had normally developed eyes. Overall photoreceptor densities were comparatively low (95,000–150,000/mm^2 in *C. magellanicus*, 110,000–200,000/mm^2 in *C. talarum*), and cone proportions were rather high (10–31% and 14–31%, respectively). The majority of cones expressed the middle-to-longwave-sensitive (L) opsin, and a 6–16% minority expressed the shortwave-sensitive (S) opsin. In both species the densities of L and S cones were higher in ventral than in dorsal retina. In both species the tuning-relevant amino acids of the S opsin indicate sensitivity in the near UV rather than the blue/violet range. Photopic spectral electroretinograms were recorded. Unexpectedly, their sensitivity profiles were best fitted by the linear summation of three visual pigment templates with λ_{max} at 370 nm (S pigment, UV), at 510 nm (L pigment), and at 450 nm (an as-yet unexplained mechanism). Avoiding predators and selecting food during the brief aboveground excursions may have exerted pressure to retain robust cone-based vision in *Ctenomys*. UV tuning of the S cone pigment is shared with a number of other hystricomorphs. J. Comp. Neurol. 518:4001–4015, 2010.

INDEXING TERMS: subterranean rodents; retinas; electroretinogram; cone photoreceptors; color vision

Several lineages of mammals comprising more than 300 extant species have adopted a subterranean or fossorial lifestyle (Nevo, 2000). These species, belonging to 10 families representing four mammalian orders, spend most of their lives in dark burrow systems, characterized by a low food supply and distinctive environmental conditions such as high humidity, limited ventilation, hypoxic and hypercapnic conditions (Buffenstein, 2000; Burda et al., 2007), and without most of the sensory cues existing aboveground (Nevo, 2000; Kimchi and Terkel, 2001; Burda, 2003). This stable and predictable but stressful environment had an enormous effect on the animals inhabiting it. As a consequence, subterranean mammals have converged in many morphological and physiological traits in response to similar selection pressures, but have diverged in others by adjustments to local habitat characteristics (Burda, 2003).

In subterranean rodents the permanent darkness in the underground tunnels led to reductions in sight and hypertrophies of other sensory systems, including olfaction, vocalization, taste, and touch (Nevo, 2000; Burda, 2003), although the level of regression or hypertrophy depends on the degree of fossoriality. Concerning the visual system, one of the most prominent features in some subterranean rodents is the reduction of eye structures and the apparent blindness (Nevo, 2000; Burda, 2003;

Grant sponsor: Comision Nacional de Investigacion Cientifica y Technologica (CONICYT); Grant number: PBCT-CONICYT ACT45 (to A.G.P.); Grant sponsor: Consejo Nacional de Investigaciones Cientificas y Técnicas; Grant number: PIP 5670 CONICET (to C.E.S.).

*CORRESPONDENCE TO: Cristian E. Schleich, Laboratorio Ecofisiología, Facultad de Ciencias Exactas y Naturales, Universidad Nacional de Mar del Plata, Argentina. E-mail: cschleic@mdp.edu.ar

Received December 26, 2009; Revised April 19, 2010; Accepted May 31, 2010
DOI 10.1002/cne.22440
Published online June 17, 2010 in Wiley InterScience (www.interscience.wiley.com).

Nemec et al., 2004). *Nannospalax ehrenbergi,* one of the species that shows the most extreme adaptations to life underground, has an atrophied subcutaneous eye with a degenerate optical apparatus (Cooper et al., 1993). While electrophysiological and behavioral studies showed that *N. ehrenbergi* has lost its visual capabilities (Rado et al., 1992), its eye seems to have a role in circadian photoreception (Rado et al., 1991; David-Gray et al., 1998).

Studies in a broader range of subterranean species have since qualified this view by showing substantial differences in the level of eye regression (reviews: Nemec et al., 2007, 2008). The African mole-rats (Bathyergidae), a family of strictly subterranean rodents phylogenetically distant from spalacines, possess small superficial eyes with remarkably normal retinas (Nemec et al., 2004; Peichl et al., 2004; Mills and Catania, 2004). Two representatives, *Heterocephalus glaber* and *Fukomys anselli* (formerly *Cryptomys*), which were formerly considered blind, have been demonstrated to perceive light in behavioral studies (Hetling et al., 2005; Wegner et al., 2006).

While spalacines and bathyergids, both strictly subterranean, have lost much of their visual capabilities, the geomyids and subterranean octodontids, which show some surface activity, have retained normal eyes and vision (Burda, 2003). Both *Thomomys bottae* (pocket gopher, family Geomyidae) and *Spalacopus cyanus* (cururo, family Octodontidae) possess fully functional eyes with sizes within the normal rodent range, clear optics, and a retina conforming to the normal mammalian plan (Williams et al., 2005; Peichl et al., 2005).

South American subterranean rodents of the genus *Ctenomys* (family Ctemonyidae, suborder Hystricomorpha), have comparably normal-sized and exposed eyes. *Ctenomys* shows some aboveground activity. Members of this genus search for food within their tunnels, but most of the gathering occurs on the surface when the animals leave their burrows for short distances to cut grasses and perennial forbs, then retract into the burrows to later consume the leaves (Busch et al., 2000; del Valle et al., 2001). Therefore, despite their subterranean lifestyle, developed visual capacities seem to be necessary to select food items and avoid predators during these aboveground excursions. To date, no studies of the eye and vision in any species of the genus *Ctenomys* have been done. The objective of the present study was to determine the anatomy and function of the eye in two species of *Ctenomys*, *C. talarum* and *C. magellanicus*, two facultative but not strictly subterranean rodents that are close phylogenetically but differ in the environment that they inhabit. While *C. talarum* (belonging to the *mendocinus* group; Castillo et al., 2005) inhabits sandy soils along the Atlantic coast of Buenos Aires Province (Argentina), *C. magellanicus* (belonging to the Patagonian group) inhabits open meadows with dense grass cover, often dotted with low bushes, in the south of Argentina and Chile. Analysis of their visual capacities may elucidate whether their eye characteristics relate to different constraints set by their lifestyles and habitats and/or to their phylogeny.

MATERIALS AND METHODS

Animals

Adults of either sex of *C. talarum* (n = 3) and *C. magellanicus* (n = 5) were captured in Mar de Cobo (37°45′S, 57°56′W, Buenos Aires Province, Argentina) and in Isla Grande de Tierra del Fuego (53°18′S; 69°01′W; Chile) using live traps and were transported to the laboratory in individual plastic cages. Animals were maintained in an animal facility at the Universidad de Valparaiso with controlled photoperiod and temperature (12:12 L:D; 25 ± 1°C). The tuco-tucos were fed mixed grasses, sweet potatoes, lettuce, sunflower seeds, corn, carrots, and alfalfa ad libitum. All experimental procedures were approved by the bioethics committee of the Universidad de Valparaiso in accordance with the bioethics regulation of the Chilean Research Council (CONICYT), and complied with international regulations (DHEW Publications, NIH 80-23).

Retinal histology and opsin immunocytochemistry

The eyes of *C. magellanicus* and *C. talarum* were obtained directly after killing the animals by a lethal dose of diethyl ether or halothane. The eyes were marked at their dorsal pole for orientation, enucleated, punctured at the corneal rim for better fixative penetration, fixed in 4% paraformaldehyde in 0.1 M phosphate-buffered saline (PBS, pH 7.4) for a minimum of 24 hours, and transferred to PBS for further handling. Eye dimensions were recorded and the retina was removed from the eyecup. For retinal morphology, pieces of retina were embedded in Epon, sectioned vertically (i.e., perpendicular to the retinal layers) at 1 μm, and stained with Toluidine blue. Immunocytochemistry was performed on whole retinas or frozen sections. The tissue was cryoprotected by successive immersion in 10%, 20%, and 30% (w/v) sucrose in PBS. For staining of whole retinas the retina was repeatedly shock-frozen and thawed to improve penetration of the antibodies. For sections the retina was transferred from 30% sucrose to tissue-freezing medium (Reichert-Jung, Bensheim, Germany), sectioned vertically at a thickness of 14 μm with a cryostat, and collected on slides.

Opsin immunocytochemistry followed previously described protocols (Peichl et al., 2000, 2004). Briefly, adhering remains of the retinal pigment epithelium were bleached and the tissue was preincubated for 1 hour in PBS with 0.5% Triton X-100 and 10% normal goat serum

(NGS), or normal donkey serum (NDS) when secondary antibodies from donkey were used. Incubation in the primary antibody/antiserum solution was for 3–4 days (free-floating tissue) or overnight (sections on the slide) at room temperature. The longwave-sensitive (L) cone opsin was detected with the rabbit antiserum JH 492 (dilution 1:2,000–1:4,000), the shortwave-sensitive (S) cone opsin with the rabbit antiserum JH 455 (dilution 1:5,000), or the goat antiserum sc-14363 (dilution 1:100). The rabbit antisera were kindly provided by J. Nathans (Wang et al., 1992), the goat antiserum was purchased from Santa Cruz Biotechnology (Heidelberg, Germany). Rod opsin was detected with the mouse monoclonal antibody rho4D2 (dilution 1:500), kindly provided by R.S. Molday (Hicks and Molday, 1986). Binding sites of the primary antibodies were detected by indirect immunofluorescence, with a 1-hour incubation in Alexa goat antirabbit IgG, Alexa donkey antigoat IgG, or Alexa goat antimouse IgG, respectively. Double-labeling for L cone and S cone opsin was performed by incubating the tissue in a mixture of antisera JH 492 and sc-14363. In this case visualization was by incubation with a mixture of Cy5-conjugated donkey antigoat IgG and Alexa 488-conjugated donkey antirabbit IgG. In some retinas used for the topographical analysis of cone densities, incubation with the primary antisera was followed by an overnight incubation in goat antirabbit IgG, an overnight incubation in rabbit peroxidase-anti-peroxidase (PAP) complex, and visualization with 3,3′-diaminobenzidine (DAB) and H_2O_2. Whole retinas and retinal pieces were flattened onto slides with the photoreceptor side up. All tissue was coverslipped with an aqueous mounting medium (AquaPoly/Mount, Polysciences, Warrington, PA).

All of the above variations of the staining protocol gave consistent results. The specificity and characterization of the opsin antibodies have been described. For the rod opsin antibody rho4D2, rat rod outer segments (OS) were used as immunogen, and its epitope was mapped to the rhodopsin N-terminus (Hicks and Molday, 1986). This antibody has proven effective to specifically label rod OS in the retina of mammals. The L opsin antiserum JH 492 and the S opsin antiserum JH 455 were raised against epitopes of the human red and blue cone opsin, respectively. DNA segments encoding the last 38 amino acids of the human red cone opsin (all of which are shared by the human green cone opsin) and the last 42 amino acids of the human blue cone opsin were separately inserted into the polylinker of the T7 gene 10 expression vector pGEMEX (Promega, Madison, WI). Each cone opsin-derived peptide was produced as a carboxy-terminal extension of the T7 gene 10 protein. The fusion proteins were purified and used to immunize rabbits. Antisera were tested by immunofluorescent staining of transiently transfected tissue culture cells expressing recombinant human cone pigments. Each was observed to stain cells transfected with the corresponding cDNA clone but not untransfected cells (Wang et al., 1992). The S opsin marker sc-14363 is an affinity-purified goat polyclonal antibody raised against a 20-amino-acid synthetic peptide mapping within amino acids 1–50 of the human blue cone opsin (EFYLFKNISSVGPWDGPQYH), as determined from sequencing and mass spectrometry of its blocking peptide (Santa Cruz Biotechnology; sc-14363 P) by Schiviz et al. (2008). All these antibodies have been used in a range of mammals by various laboratories and have reliably labeled the respective photoreceptor types. The studies included various hystricomorph rodents (Bathyergidae: Peichl et al., 2004; *Octodon degus*: Jacobs et al., 2003; *Spalacopus cyanus*: Peichl et al., 2005; *Dasyprocta agouti*: Rocha et al., 2009). In *Ctenomys*, the rod opsin antibody rho4D2 labeled photoreceptor outer segments strongly, and other parts of the photoreceptor faintly. This is the typical rho4D2 labeling pattern observed in the rods of many mammals, indicating that in *Ctenomys* the labeling also is rod-specific. All cone opsin labeling was localized to photoreceptor outer segments. Controls double-labeled with the two S-specific antisera JH 455 (raised against a C-terminal epitope) and sc-14363 (raised against an N-terminal epitope) showed complete colocalization of the labels. Preadsorption of sc-14363 with the peptide against which it was raised (sc-14363P; Santa Cruz Biotechnology) resulted in no labeling. Omission of the primary antibodies from the incubation solution resulted in no staining, showing the specificity of the secondary antibodies.

Tissue was analyzed with a Zeiss Axioplan 2 microscope equipped with epifluorescence. Micrographs were taken with a CCD camera and the Axiovision LE software (Carl Zeiss Vision, Germany). The images were adjusted for brightness and contrast using Adobe Photoshop 7.0. (San Jose, CA); *Ctenomys talarum* L and S cone densities (see Fig. 5) were assessed from double-immunofluorescence micrographs taken at sample positions across the retina with a 40× objective. More elaborate maps of the distribution of all cones (labeled by a mixture of antisera JH 492 and JH 455) in *C. magellanicus*, and of the S cones (labeled by antiserum JH 455) in both species, were obtained from PAP/DAB-reacted retinas (see Fig. 6). At about 60–90 sample fields per retina, the cones were counted with a standard microscope equipped with a drawing tube, using a 63× objective (sample field size 160 × 320 μm) or a 100× objective (sample field size 100 × 100 μm or 100 × 50 μm), depending on local cell density. From these densities, isodensity lines were fitted by hand to create the maps. At selected regions, total photoreceptor (cone plus rod) densities were assessed by focusing on the photoreceptor inner segments with

differential interference contrast (DIC) optics, using a 100× objective. This provided rod densities and rod/cone ratios. Photoreceptor densities were not corrected for shrinkage, because shrinkage was negligible in the tissue mounted with the aqueous medium.

S opsin sequencing

To assess the spectral tuning of the S opsin (UV-sensitive vs. violet/blue-sensitive), we sequenced segments of the S opsin gene relevant for determining the spectral sensitivity of the visual pigment. In addition to *C. talarum* and *C. magellanicus*, we analyzed parts of the S opsin gene in two closely related species of octodontid Caviomorphs, *Octodon degus* and *Spalacopus cyanus.* Genomic DNA was extracted from ethanol-preserved muscle tissue to polymerase chain reaction (PCR)-amplify the S opsin gene from exon 1 to exon 3 using primers 5′-GGTGGGGCCCTGGGATGGGCCTCAG-3′ and 5′-ATGAAGAGGAACCAGGTGTAGTAC-3′. Reactions were conducted in 20 μL volumes on a MJ Mini Thermal Cycler (Bio-Rad, Hercules, CA) with initial denaturation at 94°C for 3 minutes, denaturation at 94°C for 30 seconds, annealing at 64°C for 45 seconds, extension at 72°C for 45 seconds for 35 cycles, followed by a final extension at 72°C for 10 minutes. A single ≈900 bp product was amplified, purified, and directly sequenced on both strands.

Spectral transmission of eye media and retinal spectral sensitivity

Animals were euthanized by exposure to halothane and corneas and lenses were rapidly dissected from the eye, after eye dimensions were measured with a digital caliper. Isolated corneas and lenses were placed in a quartz cell and transmission measurements were made using a spectrophotometer UV/VIS (Range 200–1,000 nm) at wavelengths from 300–800 nm.

The procedures, the optical system, and the electroretinogram (ERG) system have been described previously (Chavez et al., 2003; Peichl et al., 2005). The ERG was recorded under photopic conditions. Before an experiment the animals were anesthetized with halothane, followed by an intraperitoneal injection of a mixture of ketamine hydrochloride (120 mg/kg) and xylazine (4 mg/kg). A local corneal anesthetic (1% lidocaine) and a few drops of 1% atropine sulfate for pupil dilation were applied to the eye before placing the contact electrode on the cornea.

The optical system consisted of a quartz lamp (250 W; Oriel, Stratford, CT), a monochromator (1,200 lines/mm grating, 20 nm half-bandwidth; Oriel), and long-pass filters (RG540, RG630; Schott Optical Glass, Duryea, PA) to eliminate stray light and secondary emissions at short wavelengths from the monochromator. An electronic shutter (Uniblitz; Vincent Associates, Rochester, NY) set the flash duration and an optical quartz wedge (0–4 optical density) attenuated the incident number of photons. The monochromator, optical wedge, and shutter were under computer control and adjusted to deliver short 10-ms flashes at wavelengths from 300–700 nm in 20-nm steps. In order to obtain reliable ERG responses the adaptation background light intensity was set below a true photopic level. The white background light was obtained by a fiberoptic illuminator (150 W) giving 43.7 $\mu W/cm^2$ (19.4 cd/m^2) for *C. talarum* and 0.64 $\mu W/cm^2$ (4.85 cd/m^2) for *C. magellanicus* at the cornea. To improve the detection of S cone contributions to the photopic ERG (by decreasing the contributions of visual mechanisms above 500 nm), two individuals of *C. magellanicus* were adapted to a bright yellow background light while recording the spectral sensitivity of the ERG. The yellow background was obtained by adding a long-pass filter (<0.00001% transmission below 420 nm; model GG: Schott Optic Glass) to a fiberoptic illuminator, producing a background illumination of 16.6 cd/m^2 at the cornea (Chavez et al., 2003).

The ERG signals were recorded with a pair of Ag/AgCl electrodes, a ring-shaped electrode placed on the corneal surface, and a reference electrode in the head skin. Signals were amplified and low- and high-pass filtered (1 kHz and 1 Hz) with a high-gain amplifier (model DP-301; Warner Instruments, Hamden, CT). The ERG response was evoked by an increasing number of photons per flash (with 1–2-second intervals between the flashes) at fixed wavelength(s). The response b-wave amplitudes were measured between baseline and peak. For comparison, the amplitude response functions obtained from different individuals were normalized using a Hill equation $r/r_{max} = i / i + \sigma$, where i is the incident photon number at the cornea, r/r_{max} is the normalized b-wave response, and σ is the half-saturating response. In the spectral sensitivity experiments, the amplitude of the b-wave was determined as the average response to dim flashes ($n = 10$–50), covering the range of 330–700 nm. The spectral sensitivity function (S_λ) corresponds to $= r_{peak} / i$, where i is the flash photon flux, and r_{peak} is the b-wave maximum peak response for a dim flash.

Modeling the ERG

To interpret the ERG in terms of the contribution of visual mechanisms we used an iterative fitting procedure (built in Mathematica Software) (see Herrera et al., 2008) that combines numerical visual templates including the α- and β- absorption bands (Stavenga et al., 1993; Palacios et al., 1998; Govardovskii et al., 2000). The λ_{max} of the β-band was estimated as β-band $\lambda_{max} = 123 + 0.429$ λ_{max} α-band (Palacios et al., 1998). Therefore, the spectral response of the ERG is reproduced by:

TABLE 1.

Eye and Retina Dimensions in *Ctenomys talarum* and *Ctenomys magellanicus*

	Ctenomys talarum	*Ctenomys magellanicus*
Eye dimensions		
Axial length (mm)	5.5 – 6.0 (mean 5.7; n = 5)	7
Equatorial diameter (mm)	5.5 – 6.0 (mean 5.8; n = 5)	7
Cornea diameter (mm)	4.3 – 4.6 (n = 2)	5.4
Lens diameter (mm)	3.6 – 3.7 (n = 5)	4.4 – 4.7 (n = 3)
Lens thickness (mm)	2.8 – 3.0 (n = 5)	3.2 – 3.7 (n = 3)
Retina		
Diameter (mm)	9.5 – 10.0 (n = 3)	12.0 – 13.0 (n = 2)
Thickness (μm)[1]	~120 – 160	~150
Number of ONL tiers[1]	3 – 4	4
Number of INL tiers[1]	2 – 3	3

n, number of eyes or retinas analyzed.
[1]Thickness of the retina and its layers decreases from center to periphery.

$$P_{ERG(\lambda)} = \sum_{i=1}^{n} k_i p_i \quad (1)$$

where n is the number of different photoreceptor types, i their corresponding index, k_i their relative contribution, and p_i their respective absorption spectrum. The long-wavelength increase in sensitivity by self-screening for axial absorbance (van Roessel et al., 1997) was ignored in our analysis.

RESULTS

Eye dimensions, cornea, and lens spectral transmission

The eyes of both *Ctenomys* species were nearly spherical in shape, with an axial length of 5.7 mm and an equatorial diameter of 5.8 mm in *C. talarum* and 7/7 mm in *C. magellanicus* (Table 1). All ocular structures, including the retina, were somewhat larger in *C. magellanicus* than in *C. talarum* (Table 1; see also Fig. 6). Individual size differences within each species were also observed; they are probably related to age differences. The lenses of both species had a rather high thickness-to-diameter ratio. Transmission measurements of lenses of both species are shown after normalization at 700 nm in Fig. 1. It is noteworthy that in both species the lens had a very low optical transmission, with a maximum of 13–15% between 700 and 750 nm. The corneas were more transmissive. That of *C. talarum* had a maximal transmission of 65–70% between 700–800 nm, whereas that of *C. magellanicus* showed only 35–40% transmission at these wavelengths. While in both species the spectral transmission of lenses and corneas dropped rapidly below 400 nm, there still was some transmission in the near-UV range around 350 nm, with *C. magellanicus* and *C. talarum* still exhibiting 60% and 40% of their maximum transmission at 350 nm, respectively.

Retinal structure and photoreceptor types

Transverse sections of the retinas of *C. talarum* and *C. magellanicus* are shown in Fig. 2A,B. The retinas of both species are well-structured, consistent with the typical mammalian pattern. The retina of *C. magellanicus* (Fig. 2B) appears thicker, but this is not significant as thickness changes with retinal location (Table 1). The section of *C. magellanicus* is from a more central region, as evidenced by the thicker optic nerve fiber layer. The outer (ONL) and inner nuclear layers (INL) of both species contained approximately the same numbers of rows of somata (Table 1). The retinas of both species had a rather thin ONL, indicating a low packing density of photoreceptors. Indeed, photoreceptor densities measured in flattened retina were only 110,000–200,000/mm^2 in *C. talarum* (compare Fig. 4), and 95,000–150,000/mm^2 in *C. magellanicus*.

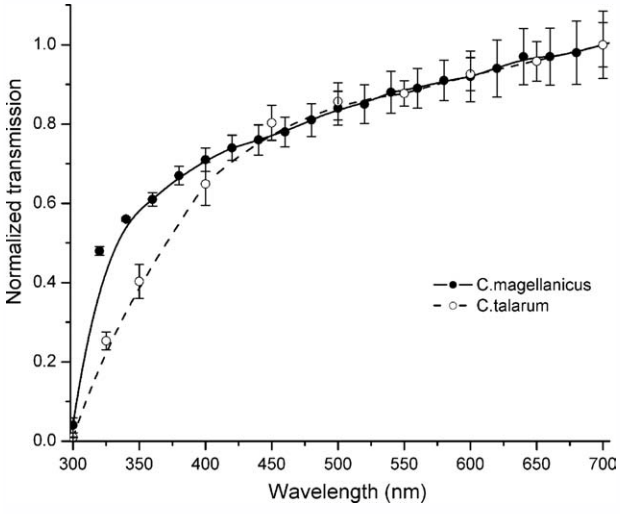

Figure 1. Normalized lens transmission (mean ± SD) in *Ctenomys talarum* (n = 6) and *Ctenomys magellanicus* (n = 3).

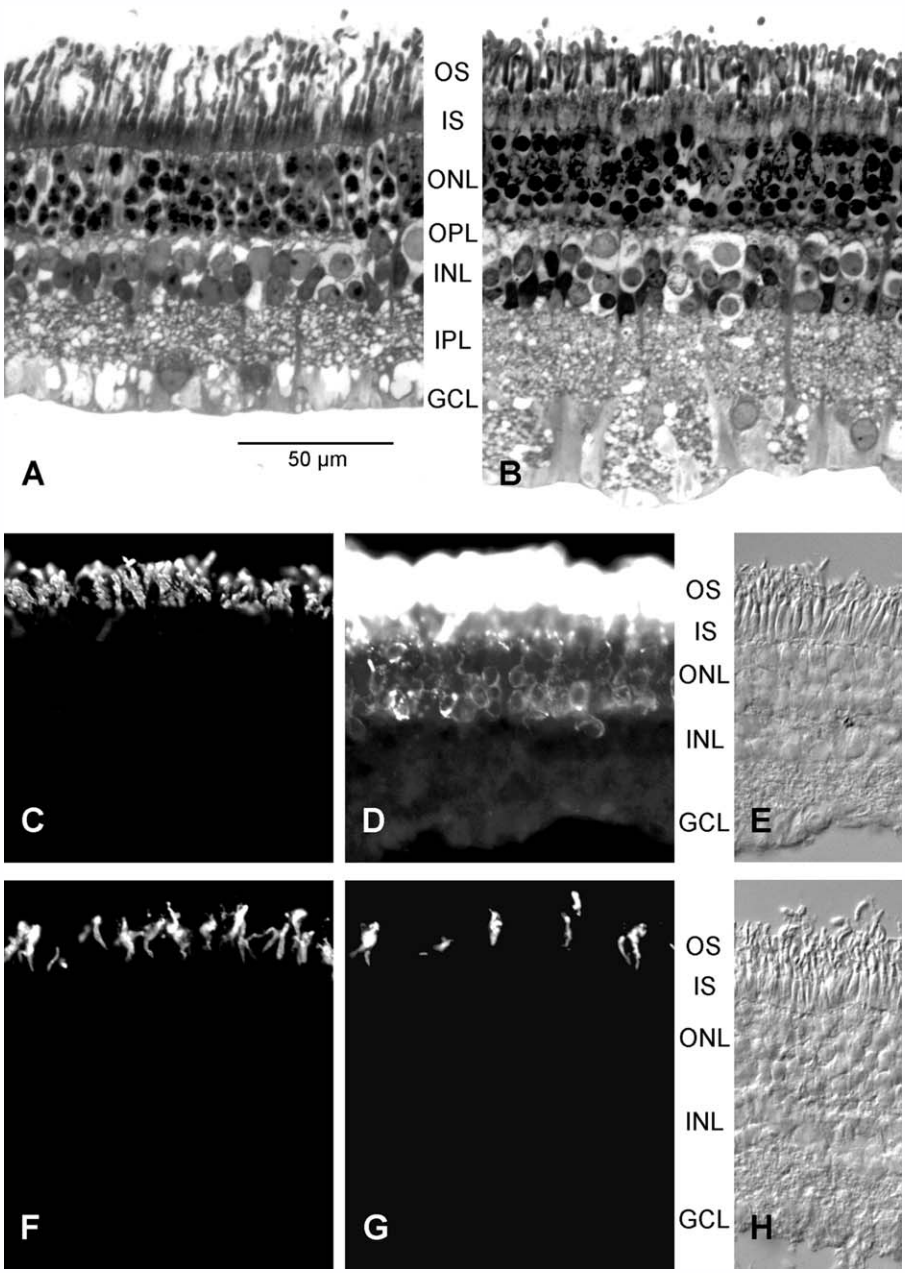

Figure 2. *Ctenomys* retinal morphology and photoreceptors. **A,B:** Transverse 1-µm sections stained with Toluidine blue to show the retinal layers in *C. talarum* (A) and *C. magellanicus* (B). Retinal thickness in both species changes with retinal location. B shows a more central location than A, as evidenced by the thicker optic nerve fiber layer below the ganglion cells. **C:** Transverse cryostat section of *C. talarum* immunolabeled for rod opsin, revealing a dense population of rod outer segments. **D:** Same field as C, overexposed to show the fainter immunoreactivity of the rod somata. **E:** Phase image of part of the field in C,D to show the retinal layers. **F–H:** Transverse cryostat section of *C. talarum* double-immunolabeled for L cone opsin (F) and S cone opsin (G), showing the outer segments of a substantial L cone population and a sparser S cone population. H: Phase image of part of the field in F,G. OS, IS, photoreceptor outer and inner segments; ONL, outer nuclear layer; OPL, outer plexiform layer; INL, inner nuclear layer; IPL, inner plexiform layer; GCL, ganglion cell layer. Scale bar in A applies to all images.

Opsin immunocytochemistry of the retina of *C. talarum* revealed the presence of rods (Fig. 2C,D) and of two types of cone (Figs. 2F,G, 3). Rods formed the majority of the photoreceptors (88,000–160,000/mm^2; Figs. 4, 5A). Their density showed no large variations across the retina, with lower values in the dorsal and ventral periphery (Fig. 5A). Albeit rod-dominated, the retina of this subterranean rodent also contained a relatively high density of cones (18,400–50,400/mm^2, representing 14–31% of all photoreceptors; Fig. 5B,C). Cone density decreased from

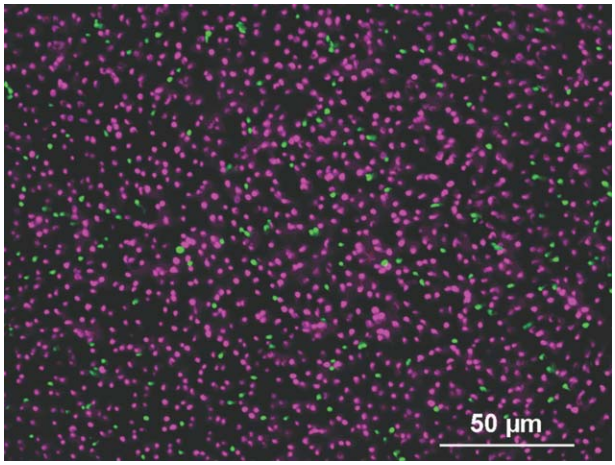

Figure 3. (color). Micrograph of L cones (magenta) and S cones (green) in the flatmounted *C. talarum* retina. Double immunofluorescence with L and S opsin antibodies, showing the density and proportion of the two cone types and the absence of opsin coexpression.

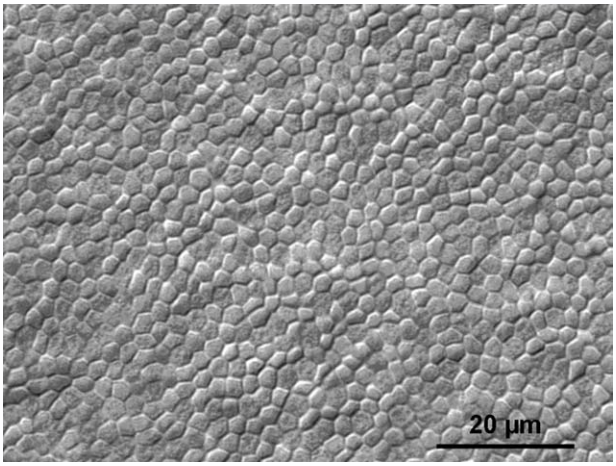

Figure 4. Phase image of part of the field in Fig. 3 at higher magnification to show the density of all photoreceptors (rods and cones).

central to peripheral retina, with the lowest densities in dorsal and nasal periphery. The majority of cones expressed the L opsin and a minority the S opsin. Coexpression of the two opsins was not observed in any cones: each cone was either a pure L or a pure S cone (Fig. 3). The L cones had densities of 19,000–47,500/mm^2, with higher densities in central and ventral retina, and lower densities in dorsal periphery (Fig. 5D). The density range of S cones was 1,800–7,300/mm^2, representing 5.7–16.5% of all cones (Fig. 5E,F). S cone densities were highest in ventral retina and dropped toward dorsal periphery (Fig. 6C).

Opsin labeling of the retina of *C. magellanicus* showed the same qualitative properties but some quantitative differences. Rod densities were overall lower (80,000–123,000/mm^2), with highest densities along the horizontal meridian and lowest densities in ventral retina. Cone densities were high (10,500–47,000/mm^2, representing 10–31% of all photoreceptors). Cone density peaked in central retina slightly nasal to the optic nerve head and dropped more strongly toward the dorsal than ventral periphery (Fig. 6A). In *C. magellanicus* too, L opsin-expressing cones formed the majority and S opsin-expressing cones a minority (9–25% of all cones), coexpression of both opsins was not observed. S cone density (1,200–8,700/mm^2) peaked slightly ventral to the optic nerve head and dropped more strongly toward the dorsal than ventral retina (Fig. 6B). Local comparison of total cone density (Fig. 6A) and S cone density (Fig. 6B) allowed extrapolation of the L cone density distribution. It largely followed the distribution of all cones, with a central peak of 43,000/mm^2 slightly nasal to the optic nerve head and a minimum of 8,000/mm^2 in dorsal periphery. As the S cone density peak did not colocalize with the cone density peak (Fig. 6A,B), highest S cone proportions of 20–25% were present at the S cone peak, across the ventral retina, and in the dorsal periphery. Lowest S cone proportions of around 10% were present in the region of maximal total cone density, in temporal and nasal midperiphery and periphery, and in dorsal midperiphery.

Comparison of the cone populations in *C. talarum* and *C. magellanicus* reveals a similar trend to higher densities of both cone types in ventral retina. However, there are noteworthy differences in topographic distribution, particularly that of the S cones (compare Fig. 6B,C).

Opsin sequence

The S opsin gene sequence of *C. talarum* and *C. magellanicus* revealed the presence of those amino acids that have a crucial role in shifting the spectral sensitivity of the S pigment toward the UV range (Phe at site 86, Thr at site 93, and Ala at site 97; Table 2). For comparison, we also partially sequenced the S opsin gene in the Octodontidae species *Octodon degus* and *Spalacopus cyanus*. Besides small differences in other amino acids, both *Ctenomys* species and Octodontids showed the same amino acids at the tuning relevant sites, as is also the case for *Mus musculus*, suggesting a UV tuning of the S cone pigment in these Caviomorph rodents. Sequence details have been deposited in GenBank (accession numbers: *Ctenomys magellanicus*, GU830972; *Ctenomys talarum*, GU830973; *Octodon degus*, GU830970; *Spalacopus cyanus*, GU830971).

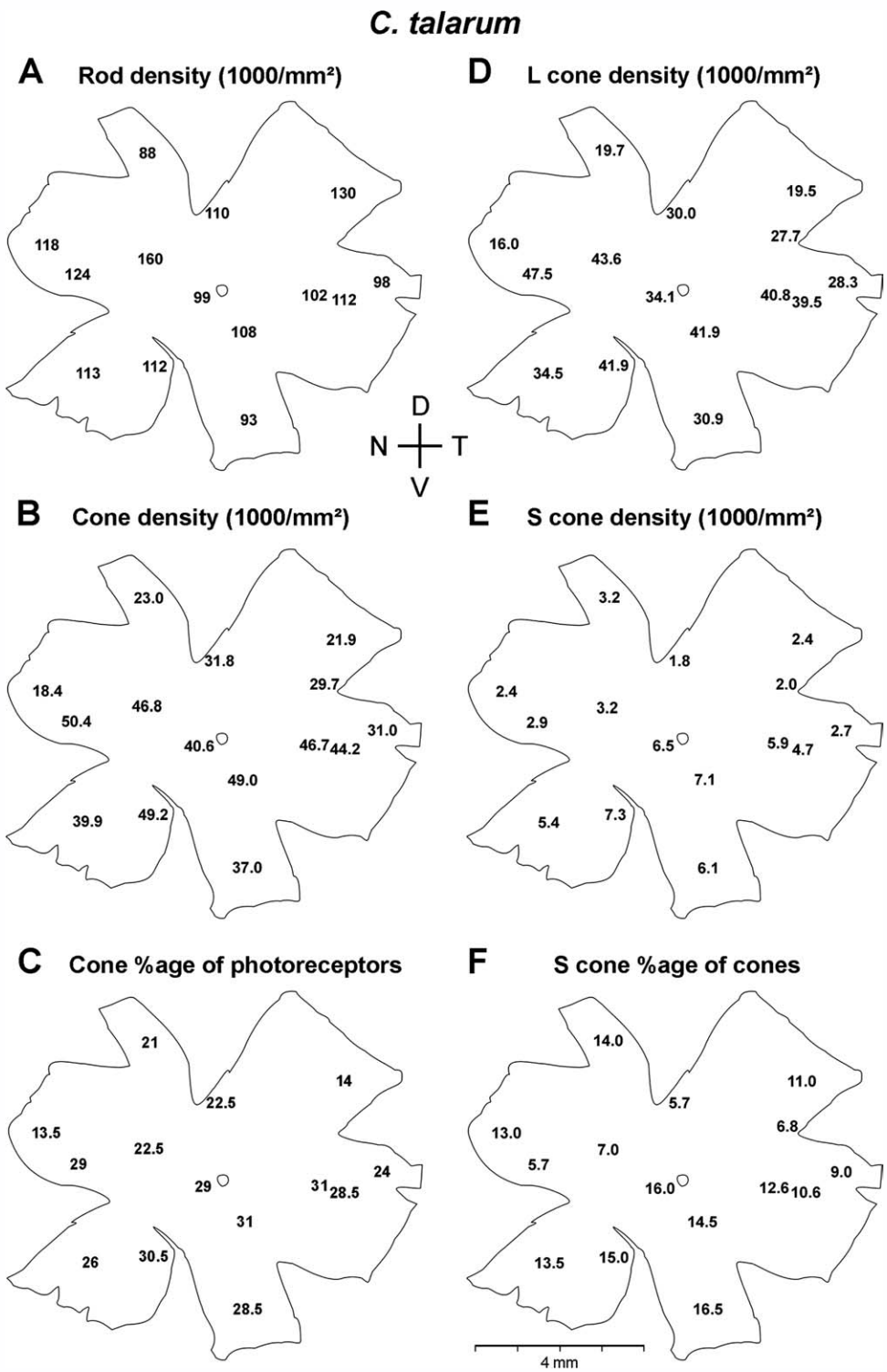

Figure 5. Maps of photoreceptor densities and proportions in *C. talarum* (six maps of the same retina) showing rod density (A), total cone density (B), cone percentage of photoreceptors (C), L cone density (D), S cone density (E), and the S cone percentage of cones (F). The small circle in the center of the retina indicates the optic nerve head. D, dorsal; V, ventral; N, nasal; T, temporal.

Retinal spectral sensitivity

Figure 7A shows the changes in sensitivity during dark adaptation for two individuals of *C. talarum*. The increase in sensitivity, over the measured time span of 25 minutes, was about 0.5 log units and thus relatively modest compared to that in other rodents. In the related subterranean coruro, the sensitivity after 25 minutes in the dark increases by 2 log units (Peichl et al., 2005), and the

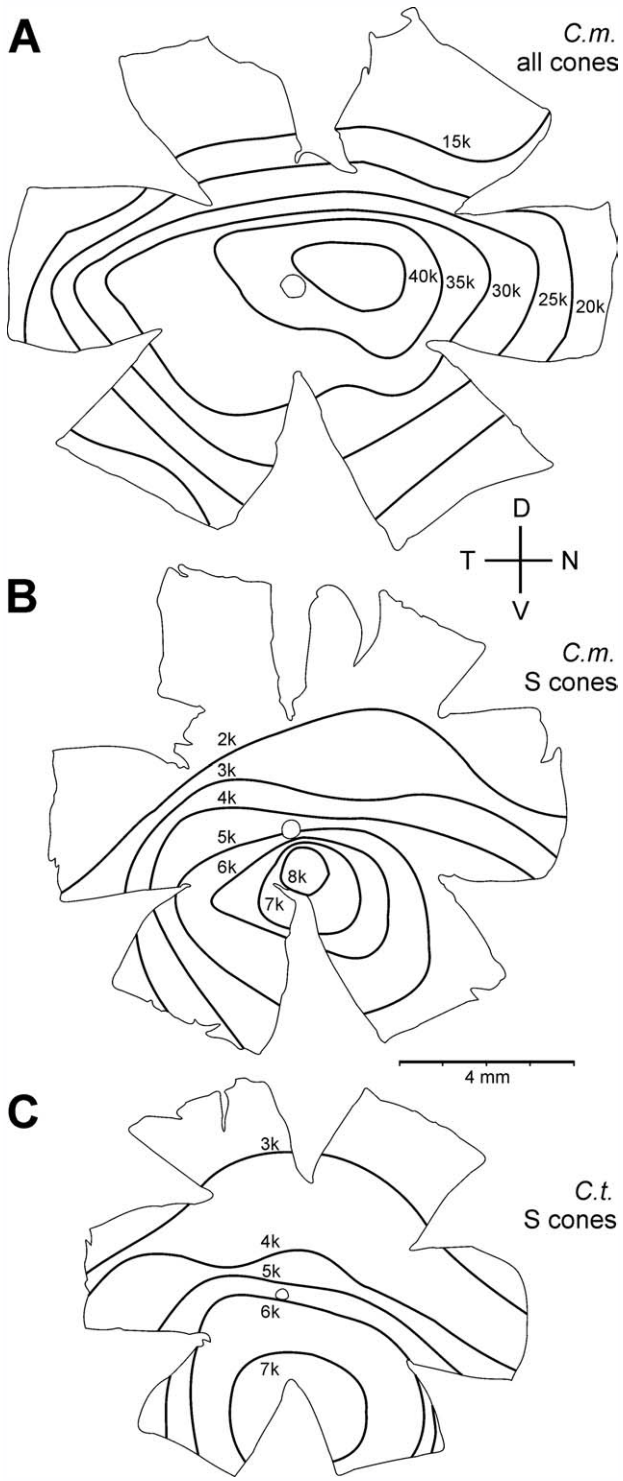

Figure 6. Topographic maps of the density distribution of all cones (**A**) and of S cones (**B**) in *C. magellanicus*, and of S cones (**C**) in *C. talarum*. Densities at the isodensity lines are given in 1,000/mm^2. Small circles in the center of the retinas indicate the optic nerve head. Orientation (D, V, T, N) and scale apply to all retinas.

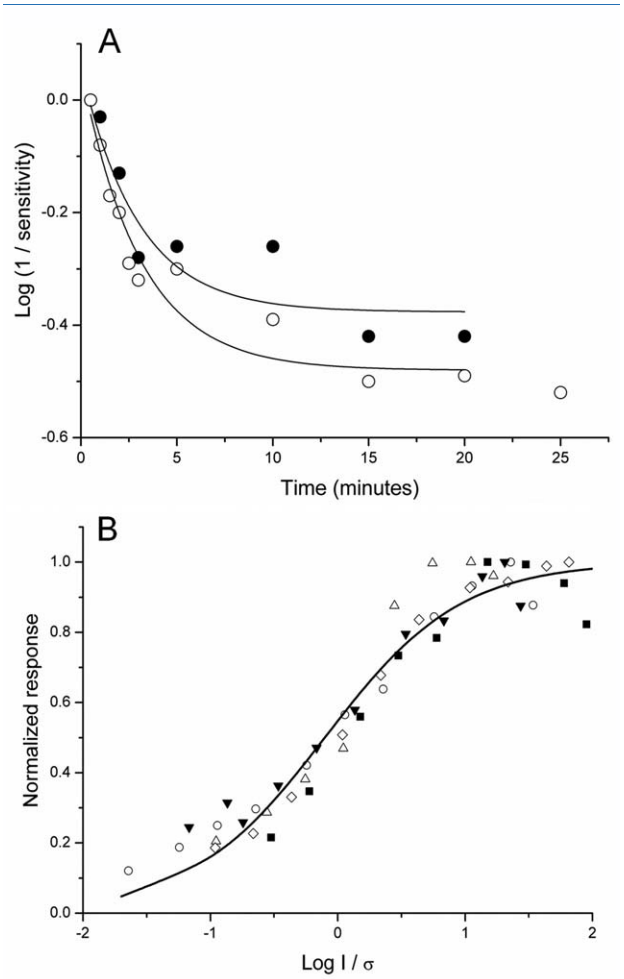

Figure 7. **A:** Dark adaptation functions for two *C. talarum* individuals. Time zero corresponds to light off after a photopic adaptation. Stimuli (n = 5 on average) were monochromatic flashes (λ = 500 nm, flash duration 5 ms) of decreasing intensities. The continuous lines are the individual best fits using an exponential decay function. **B:** Normalized b-wave intensity response function of *C. magellanicus* (λ = 500 nm, 10 ms flashes, n = 5). Different symbols correspond to different individuals. The continuous line is a best fit using a Hill equation from the ORIGIN statistics package.

increase is similarly high in *Octodon bridgesis*, a nocturnal species from South America (Chavez et al., 2003). Figure 7B shows a normalized ERG b-wave intensity response function for *C. magellanicus*. The continuous line is the best fit to the data using a Hill equation (see Materials and Methods). The response increases as a linear function of intensity until reaching a saturating plateau, which is a general mammalian feature. The normalized photopic S_λ responses of individuals of both species, after correction for lens spectral absorption, are shown in Fig. 8. The responses of both species had two main peaks of sensitivity, one at about 500 nm and the other at 440–450 nm in *C. talarum* and at 450–460 nm in *C. magellanicus*.

TABLE 2.

S Cone Opsin Amino Acids of *Mus musculus*, *Octodon degus*, *Spalacopus cyanus*, *Ctenomys magellanicus*, *Ctenomys talarum,* and *Cavia porcellus*

Species	λ_{max} (nm)	46	49	52	81	*86*	90	*93*	*97*	114
M. musculus[1]	359	Phe	Phe	Thr	Leu	Phe	Ser	Thr	Ala	Ala
*O. degus**,[2]	360	–	–	–	–	–	–	–	–	–
*S. cyanus**,[3]	365	–	–	–	–	–	–	–	–	–
*C. magellanicus**	370	–	–	–	–	–	–	–	–	–
*C. talarum**	370	–	–	–	–	–	–	–	–	–
C. porcellus[4]	400	Ile	Cys	–	–	Val	–	Ala	–	Gly

UV tuning codons underlaid in gray shades. Amino acid numbers according to bovine rod opsin nomenclature (46 bovine rho = 41 mouse S cone opsin). Italic numbers represent amino acids important in spectral tuning, Dashes indicate amino acids identical to mouse. GenBank accession numbers: *Mus musculus* NM_007538, *Octodon degus* GU830970, *Spalacopus cyanus* GU830971, *Ctenomys magellanicus* GU830972, *Ctenomys talarum* GU830973, *Cavia porcellus* AY552608.

Data sources: *present study; [1]Yokoyama et al. (1998); [2]Chávez et al. (2003); [3]Peichl et al. (2005); [4]Parry et al. (2004).

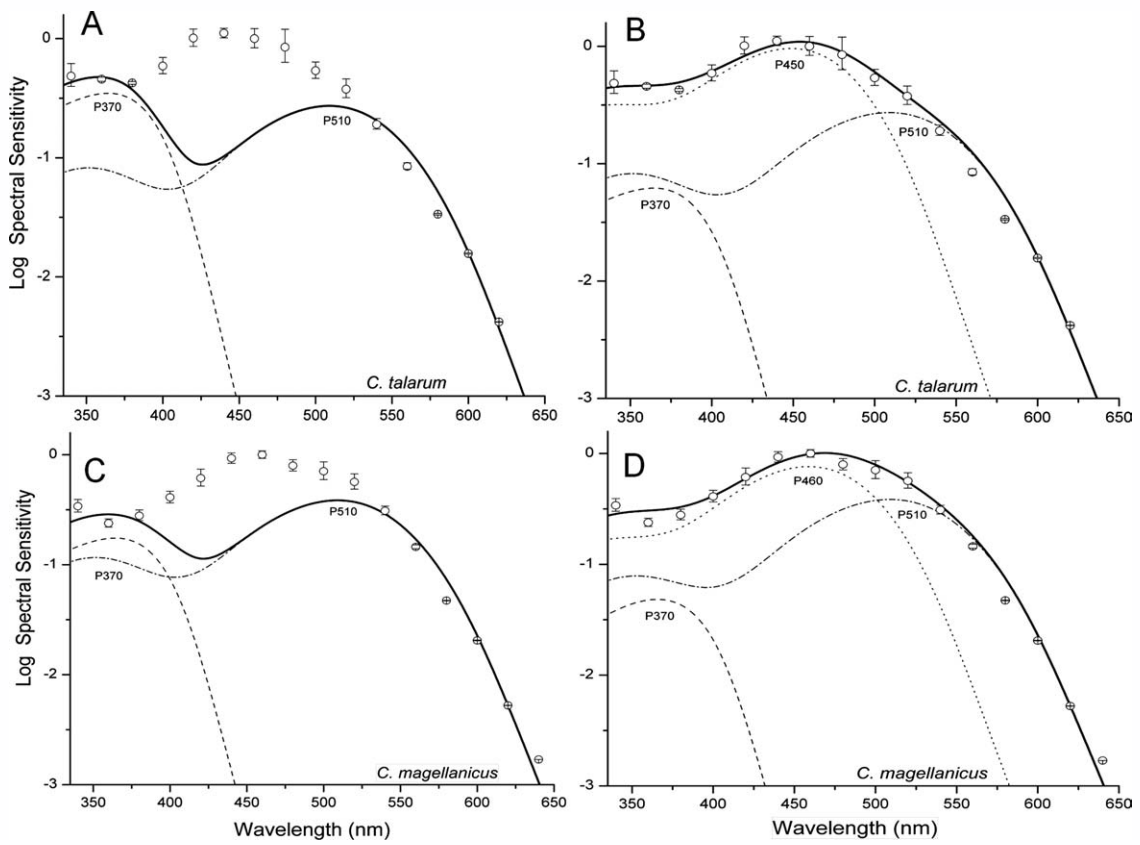

Figure 8. Photopic spectral sensitivity functions of *C. talarum* (**A,B;** n = 3) and *C. magellanicus* (**C,D;** n = 5), assessed from the ERG b-waves. Maximum sensitivity is normalized to 1 (open circles and bars give mean ± SEM). The visual pigment absorption function (thick solid line) was modeled by the linear summation of two cone visual pigment templates with maximal sensitivity at λ_{max} = 370 nm (dashed line) and λ_{max} = 510 nm (dash-dotted line) in A,C, and by addition of a putative third visual pigment template with λ_{max} = 450 and 460 nm (dotted line), respectively, in B,D.

C. magellanicus presented a further sensitivity peak in the UV range, which is not so obvious in *C. talarum* (but see below).

To uncover the possible cone mechanisms underlying the photopic S_λ, we used an interactive model fitting (see Materials and Methods) to the data combining different visual templates in order to specify more accurately the spectral position of the cone pigments. Contrary to our expectations from the immunocytochemical results, the combination of two cone visual pigment templates with peaks at 370 nm (S cone, near UV) and at 510 nm (L cone) did not produce a good fit with the S_λ curve (Fig. 8A,C). Only the linear summation of three visual pigment absorption functions with peaks at 370 nm, 440 nm, and

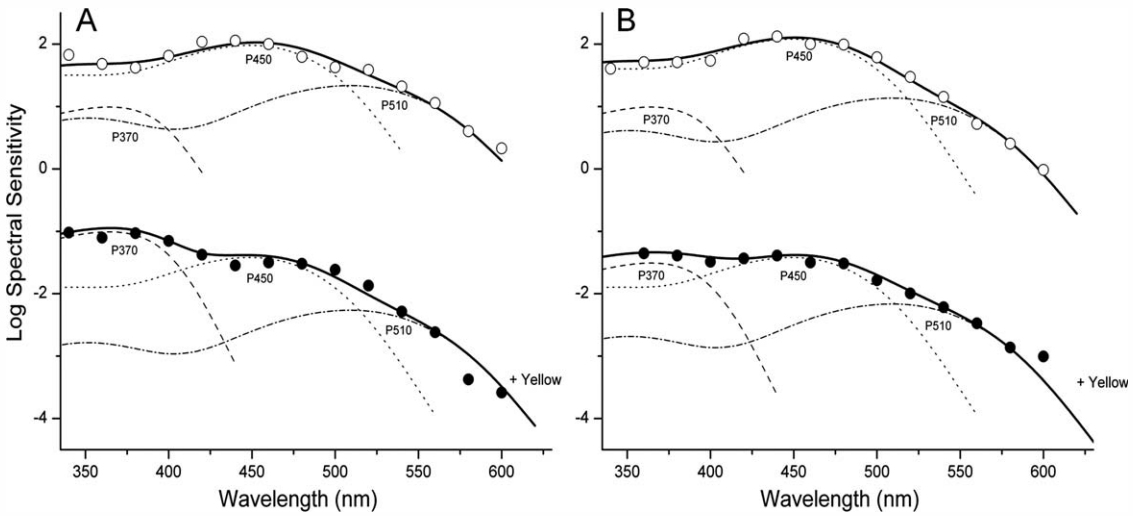

Figure 9. Photopic spectral sensitivity with white light adaptation (upper curves) and with yellow adaptation (lower curves) in two individuals of *C. talarum* (left: animal **A**; right: animal **B**). The thick solid line represents the sum of three visual pigment templates with λ_{max} = 370 nm, λ_{max} = 450 nm, and λ_{max} = 510 nm as in Fig. 8B. The curves for white adaptation and yellow adaptation were shifted arbitrarily on the ordinate. The weightings in the contribution of the three templates are for A (upper) P370 (8%), P450 (76%), P510 (17%) and B (upper) P370 (7%), P450 (84%), P510 (9%). For the yellow adaptation condition for A (lower) P370 (69%), P450 (27%), P510 (4%) and B (lower) P370 (40%), P450 (51%), P510 (9%).

510 nm produced a good fit to the average S_λ curve in both species (Fig. 8B,D). To further explore the underlying cone mechanisms we utilized a yellow adaptation background to desensitize the longwave-sensitive mechanisms (L cones and rods) and to unmask any possible shortwave sensitivity. The results again support the participation of a UV-sensitive S cone mechanism, an L cone mechanism, and an—as-yet unexplained—contribution of a third mechanism with a peak at 440–460 nm (Fig. 9).

DISCUSSION

Because of the permanent darkness in subterranean burrows, vision was supposed to be useless in this habitat. The regression of some visual structures observed in the blind mole-rat gave preliminary support to this hypothesis (Sanyal et al., 1990, Cooper et al., 1993). However, the extension of studies to other species of subterranean rodents have revealed a different picture, with the level of regression or development of visual structures depending on the degree of attachment of the species to subterranean life (Peichl et al., 2004, 2005; Williams et al., 2005). There appears to be a continuum of visual capabilities across species, with the extremes of reduced or absent visual structures in some strictly subterranean species (e.g., *S. ehrenbergi*, Cooper et al., 1993), and functional eyes in species displaying regular aboveground activity (e.g., *Thomomys bottae, Spalacopus cyanus*; Williams et al., 2005; Peichl et al., 2005). The results of the present work demonstrate that the members of the genus *Ctenomys* belong to the latter group.

Eye size, which is a good predictor of visual capabilities, was shown to vary across subterranean species (Nemec et al., 2007). While *S. ehrenbergi* and *Talpa europaea* have reduced eyes (even positioned subcutaneously in the former species; Cooper et al., 1993; Glösmann et al., 2008), the eyes of the two *Ctenomys* species analyzed here are normally developed and have similar dimensions to those of surface-dwelling rodents of comparable size (Howland et al., 2004). This suggests a normal image formation capacity in the *Ctenomys* retina. The lenses of *Ctenomys* exhibit a very low spectral transmission between 400–700 nm, compared to other subterranean rodents, like *S. cyanus* and *T. bottae*, whose lenses and corneas show little absorption of light for wavelengths in that range (Peichl et al., 2005; Williams et al., 2005). Since *Ctenomys* individuals move from total darkness to bright light during their aboveground excursions, it is possible that the low spectral transmission of their lens could act as a protective filter against retinal damage caused by bright light exposure after being dark-adapted in their burrows. Another consequence of low transmission lenses is that very modest changes in the increase of sensitivity were observed in our dark-adaptation conditions. However, the time window of our recordings was relatively short due to the effective period of anesthesia. This also precluded further exploration of other scotopic functions in *Ctenomys*. A larger sample of lenses will have to be measured to corroborate the

present transmission data and to exclude pathologies (e.g., an early form of cataract in some individuals). Irrespective of this caveat, it can be stated that *Ctenomys* lens transmission, particularly that of *C. magellanicus*, allows near-UV light to reach the retina. Concerning the interspecific differences in transmission values, it seems that the greater transmissivity of the *C. magellanicus* lens, together with the higher sensitivity peak in the UV range observed in the retina of this species in comparison with *C. talarum*, provides some support for a greater capacity of *C. magellanicus* to obtain and use visual signals in this spectral range.

The retinas of *C. talarum* and *C. magellanicus* are normally developed and their morphology conforms to the general mammalian pattern. This has also been found in other species of subterranean rodents (Cernuda-Cernuda et al., 2002; Peichl et al., 2004, 2005; Williams et al., 2005; Nemec et al., 2008). However, there are some differences across species in the density of photoreceptors. *Ctenomys talarum* and *C. magellanicus* have 110,000–200,000 and 95,000–150,000 photoreceptors/mm^2, respectively. Similar densities are present in the bathyergids *F. anselli* and *F. mechowii* (100,000–150,000/mm^2; Peichl et al., 2004). The photoreceptor densities of the pocket gopher and the European mole are even lower (70,000–125,000/mm^2 and ≈100,000/mm^2, respectively; Williams et al., 2005; Glösmann et al., 2008), whereas those of *S. cyanus* are somewhat higher (160,000–224,000/mm^2; Peichl et al., 2005).

Like most mammalian retinas, those of both *Ctenomys* species are rod-dominated. Rod densities roughly correlate with an animal's lifestyle, being higher in nocturnal species than in diurnal ones (review: Peichl, 2005). The rod densities of 88,000–130,000/mm^2 in *C. talarum* and 80,000–123,000/mm^2 in *C. magellanicus* are below the mammalian average (200,000–400,000/mm^2) and markedly lower than in nocturnal surface dwellers (up to about 700,000/mm^2 in the African pouched rat; Peichl and Moutairou, 1998). Unexpectedly low rod densities were also observed in other subterranean rodents and insectivores (e.g., *T. bottae* 55,000–100,000/mm^2; *F. anselli* 100,000–150,000/mm^2; *T. europaea* 130,000–140,000/mm^2) whose less densely packed rods frequently have larger sizes (Peichl, 2005; Nemec et al., 2007). While the low density of rods in strictly subterranean rodents may be caused by the lack of selective pressure to maintain and optimize scotopic vision in a completely lightless habitat, it is not clear why facultative subterranean species that display aboveground activity also at night, like *Ctenomys*, similarly exhibit low densities of the rods that would be useful during nocturnal surface excursions.

Although rod-dominated, the retinas of both *Ctenomys* species feature a high proportion of cones (14–31% in *C. talarum*, 10–31% in *C. magellanicus*). This pattern was also observed in other species of facultative subterranean rodents like *T. bottae* (≈25%; Williams et al., 2005) and *S. cyanus* (10%; Peichl et al., 2005). These cone proportions are lower than in some diurnal mammals, but higher than in nocturnal surface-dwelling species (0.5–3% cones; Peichl et al., 2000; Nemec et al., 2007). This supports the view that the *Ctenomys* photoreceptor arrangement has adapted to photopic vision during their aboveground activity and not to vision in the dark burrows. A number of other fossorial rodents, particularly burrowing species that forage substantially aboveground also during daylight, have similarly high cone proportions (see above). An extreme case is the burrowing sciruids, where cones dominate (e.g., 85% cones in the California ground squirrel; Kryger et al., 1998). Indeed, during aboveground excursions such species have to rely largely on vision to detect predators. For example, analysis of their various and specific warning calls has shown that prairie dogs can identify different predators and even different predator colors (Kiriazis and Slobodchikoff 2006; Slobodchikoff et al., 2009). Further burrowing mammals are known to distinguish between terrestrial and aerial predators by different warning calls (for references, see Kiriazis and Slobodchikoff, 2006). It remains to be shown that tuco-tucos have similar capabilities.

Most nonprimate mammals possess two spectrally distinct classes of cone pigments encoded by distinct opsin gene families (Jacobs et al., 1993; Bowmaker, 2008). The tuning of mammalian L cones usually ranges from 495–560 nm, with rodents displaying a λ_{max} between 495 nm and 530 nm. S cones range from blue-sensitive pigments with λ_{max} as long as about 450 nm to UV-sensitive pigments with λ_{max} as short as 365 nm (Bowmaker, 2008). Generally, the L cones form a majority of 85–95%, and both cone types display a centro-peripheral density gradient, with higher densities in the Area centralis and lower ones in the retinal periphery (review: Peichl, 2005). Two types of cone opsins were also detected in *Ctenomys* retinas, with L opsin expressed in 75–95% of the cones and without coexpression of L and S opsins in any cones. The densities of both cone types decreased from central to peripheral retina, with higher cone densities maintained in ventral than dorsal retina. Even though this distribution conforms to the general mammalian pattern, it is not representative for the arrangement of L and S cones among subterranean rodents. While the phylogenetically related *S. cyanus* has a similar array of cones (Peichl et al., 2005), the vast majority of cones in the African mole-rats express the S opsin (most of them coexpressing low levels of L opsin), and only about 10% of the cones express L

opsin exclusively (Peichl et al., 2004). On the other extreme, the blind mole-rat has functional L cones but no functional S cones (David-Gray et al., 2002). This may indicate evolutionary adaptations to different species-specific visual needs (Nemec et al., 2007) or the absence of selective pressure toward a particular kind of photoreceptor distribution.

As noted above, the mammalian S cone pigment may be tuned to violet/blue or to UV. The ancestral mammalian S pigment was almost certainly UV-sensitive (Hunt et al., 2001, 2007), and several species of rodents have retained this UV tuning (for reviews, see, e.g., Jacobs, 1993, 2004; Peichl, 2005; Bowmaker, 2008). While the blue/violet-sensitive S opsins present in many mammals have Tyr or Leu at amino acid position 86, the UV-sensitive opsins have Phe at that critical site (Yokoyama, 2000). Both *Ctenomys* species have Phe at site 86, suggesting UV tuning. UV sensitivity of the S cone was also found by ERG recordings and S opsin gene sequencing in two phylogenetically related species, the cururo *S. cyanus* (Peichl et al., 2005; present study) and the semifossorial, diurnal degu *O. degus* (Chavez et al., 2003; Jacobs et al., 2003; present study), suggesting that Caviomorphs generally have retained the ancestral mammalian UV pigment. An exception is the guinea pig, which has a violet-tuned S pigment (400 nm) due to a single amino acid substitution at site 86 (Parry et al., 2004). Although the adaptive advantage of UV-sensitive vision is yet unknown, Chavez et al. (2003) suggested that it may play a role in visual communication by means of the UV reflecting urine used in scent-marking, a common behavior in most rodent species.

While the existence of different cone types can be determined by specific antibodies, assessment of their actual spectral tuning (S_λ) requires physiological studies, most commonly spectral ERG recordings. Based on the histologically identified L and S cones and the S opsin amino acid sequence of both *Ctenomys* species, the average S_λ curves recorded here were initially fitted using an interactive program (see Herrera et al., 2008) based on two visual pigment templates with λ_{max} values of 370 nm and 510 nm. However, this produced a poor fit (Fig. 8A,C). Unexpectedly, the addition of a third pigment template with λ_{max} at 450–460 nm yielded a better fit for both species (Figs. 8B,D, 9). We have no convincing explanation for this third mechanism. All rodent species studied to date, including the close *Ctenomys* relatives *O. degus* and *S. cyanus*, and in fact all nonprimate mammals, have only two spectral cone types (with the exception of a few species that lack S cones and only have L cones). Hence, it is very unlikely that *Ctenomys* has a third cone mechanism.

The recent discovery of intrinsically photosensitive retinal ganglion cells (ipRGCs) containing the photopigment melanopsin may offer an explanation (review: Berson, 2003). Melanopsin has a λ_{max} around 480 nm, which would be near the 440 nm peak in *Ctenomys*. However, it is unclear whether an ipRGC contribution would be detectable in the ERG b-wave. The b-wave reflects the response of ON bipolar cells, and the ipRGCs with their particularly late light response (Berson, 2003) should not contribute to this early, relatively fast ERG component (but see Dong and Hare, 2000). Also, the proportion of melanopsin containing ipRGCs is generally small (1–3%) in mammals, albeit somewhat higher in the blind mole-rat (Hannibal et al., 2002).

Rod input to the S cone pathway should also be considered in this context. In primate retina, a combined functional and structural study reported a sign-conserving gap junctional coupling between the AII amacrine cells of the rod pathway and the S cone bipolar cells (Field et al., 2009). If such a coupling also exists in *Ctenomys*, it could add to the S cone component of the b-wave at longer wavelengths up to 460 nm. Including this interaction in our fitting procedure resulted in a reasonable fit to the experimental S_λ curve (not illustrated). However, rod input is thought to modulate the cone pathway only in scotopic and mesopic vision, below the light levels of rod saturation. Our experiments were conducted in photopic conditions, as measured at the cornea, but the low absorption lenses of *Ctenomys* could have made these conditions mesopic at the retina. Also, *Ctenomys* rods may contribute at higher light levels than in conventional mammals, as has been shown for the rods of the related degu (Jacobs et al., 2003). Clearly, further experiments are needed to elucidate the enigmatic 450–460 nm mechanism in the *Ctenomys* S_λ curve.

In conclusion, our results show that the eyes of both *Ctenomys* species are very similar, and that they are comparable to those of sighted surface-dwelling rodents. The normally developed eyes and the significant proportion of two spectral cone types suggest that photopic vision has a functional significance in these facultative subterranean rodents. As described in the introduction, tuco-tucos perform foraging excursions on the surface to gather vegetation growing in the proximity of burrow entries (Busch et al., 2000). During this surface activity, tuco-tucos become vulnerable to aerial and terrestrial predators (Mastrangelo et al., 2009). Selecting food items and avoiding predators during these brief aboveground excursions may have exerted strong selective pressure to retain normal visual capabilities in the subterranean rodent *Ctenomys*. The pressure appears to have been similar for both species, as we found no marked differences in

their retinal properties that would indicate habitat-specific adaptations.

ACKNOWLEDGMENTS

We thank Stefanie Heynck for skilled technical assistance. We thank F. Bozinovic for providing the specimens of *C. magellanicus*. We also thank J. Nathans (Baltimore) and R.S. Molday (Vancouver) for kindly providing antibodies. During the elaboration of the article A.G.P. was a Senior Researcher associated with the INRIA-CORTEX team and CREA Ecole Polytechnique, France.

LITERATURE CITED

Berson DM. 2003. Strange vision: ganglion cells as circadian photoreceptors. TINS 26:314–320.

Bowmaker JK. 2008. Evolution of vertebrate visual pigments. Vision Res 48:2022–2041.

Buffenstein R. 2000. Ecophysiological responses of subterranean rodents to underground habitats. In: Lacey EA, Patton JL, Cameron GN, editors. Life underground. Chicago: University of Chicago Press. p 62–110.

Burda H. 2003. Adaptations for subterranean life. In: Kleiman DG, Geist V, Hutchins M, McDade MC, editors. Mammals I of Grzimek's animal life encyclopedia, vol.12. Farmington Hills, MI: Gale Group. p 69–78.

Burda H, Sumbera R, Begall S. 2007. Microclimate in burrows of subterranean rodents. In: Begall S, Burda H, Schleich CE, editors. Subterranean rodents: news from underground. Berlin: Springer. p 21–33.

Busch C, Antinuchi CD, del Valle JC, Kittlein MJ, Malizia AI, Vasallo AI, Zenuto RR. 2000. Population ecology of subterranean rodents. In: Lacey EA, Patton JL, Cameron GN, editors. Life underground. Chicago: University of Chicago Press. p 183–226.

Castillo AH, Cortinas MN, Lessa EP. 2005. Rapid diversification of South American tuco-tucos (Ctenomys; Rodentia, Ctenomyidae): contrasting mitochondrial and nuclear intron sequences. J Mammal 86:170–179.

Cernuda-Cernuda R, DeGrip WJ, Cooper HM, Nevo E, García-Fernández JM. 2002. The retina of Spalax ehrenbergi: novel histologic features supportive of a modified photosensory role. Invest Ophthalmol Vis Sci 43:2374–2383.

Chavez AE, Bozinovic F, Peichl L, Palacios AG. 2003. Retinal spectral sensitivity, fur coloration and urine reflectance in the genus Octodon (Rodentia): implications for visual ecology. Invest Ophthalmol Vis Sci 44:2290–2296.

Cooper HM, Herbin M, Nevo E. 1993. Visual system of a naturally blind microphtalmic mammal: the blind mole-rat, *Spalax ehrenbergi*. J Comp Neurol 328:313–350.

David-Gray ZK, Janssen JW, DeGrip WJ, Nevo E, Foster RG. 1998. Light detection in a blind mammal. Nat Neurosci 1: 655–656.

David-Gray ZK, Bellingham J, Munoz M, Avivi A, Nevo E, Foster RG. 2002. Adaptive loss of ultraviolet-sensitive/violet-sensitive (UVS/VS) cone opsin in the blind mole rat (*Spalax ehrenbergi*). Eur J Neurosci 16:1186–1194.

Del Valle JC, Lohfelt MI, Comparatore VM, Cid MS, Busch C. 2001. Feeding selectivity and food preference of *Ctenomys talarum* (tuco-tuco). Mamm Biol 66:165–173.

Dong CJ, Hare WA. 2000. Contribution to the kinetics and amplitude of the electroretinogram b-wave by third-order retinal neurons in the rabbit retina. Vision Res 40: 579–590.

Field GD, Greschner M, Gauthier JL, Rangel C, Shlens J, Sher A, Marshak DW, Litke AM, Chichilnisky EJ. 2009. High-sensitivity rod photoreceptor input to the blue-yellow color opponent pathway in macaque retina. Nat Neurosci 12: 1159–1164.

Glösmann M, Steiner M, Peichl L, Ahnelt P. 2008. Cone photoreceptors and potential UV vision in a subterranean insectivore, the European mole. J Vis 8:23.1–12.

Govardovskii VI, Fyhrquist N, Reuter T, Kuzmin DG, Donner K. 2000. In search of the visual pigment template. Vis Neurosci 17:509–528.

Hannibal J, Hindersson P, Nevo E, Fahrenkrug J. 2002. The circadian photopigment melanopsin is expressed in the blind subterranean mole rat, *Spalax*. Neuroreport 13: 1411–1414.

Herrera G, Zagal JC, Diaz M, Fernández MJ, Vielma A, Cure M, Martinez J, Bozinovic F, Palacios AG. 2008. Spectral sensitivities of photoreceptors and their role in colour discrimination in the green-backed firecrown hummingbird (*Sephanoides sephaniodes*). J Comp Physiol A 194:785–794.

Hetling JR, Baig-Silva MS, Comer CM, Pardue MT, Samaan DY, Qtaishat NM, Pepperberg DR, Park TJ. 2005. Features of visual function in the naked mole-rat *Heterocephalus glaber*. J Comp Physiol A 191:317–330.

Hicks D, Molday RS. 1986. Differential immunogold-dextran labeling of bovine and frog rod and cone cells using monoclonal antibodies against bovine rhodopsin. Exp Eye Res 42:55–71

Howland HC, Merola S, Basarab JR. 2004. The allometry and scaling of the size of vertebrate eyes. Vis Res 44:2043–2065.

Hunt DM, Wilkie SE, Bowmaker JK, Poopalasundaram S. 2001. Vision in the ultraviolet. Cell Mol Life Sci 58:1583–1598.

Hunt DM, Carvalho LS, Cowing JA, Parry JWL, Wilkie SE, Davies WL, Bowmaker JK. 2007. Spectral tuning of shortwave-sensitive visual pigments in vertebrates. Photochem Photobiol 83:303–310.

Jacobs GH. 1993. The distribution and nature of colour vision among the mammals. Biol Rev 68:413–471.

Jacobs GH, Rowe MP. 2004. Evolution of vertebrate colour vision. Clin Exp Optom 87:206–216.

Jacobs GH, Calderone JB, Fenwick JA, Krogh K, Williams GA. 2003. Visual adaptations in a diurnal rodent, Octodon degus. J Comp Physiol A 189:347–361.

Kimchi T, Terkel, J. 2001. Magnetic compass orientation in the blind mole rat *Spalax ehrenbergi*. J Exp Biol 204:751–758.

Kiriazis J, Slobodchikoff CN. 2006. Perceptual specificity in the alarm calls of Gunnison's prairie dogs. Behav Processes 73:29–35.

Kryger Z, Galli-Resta L, Jacobs GH, Reese BE. 1998. The topography of rod and cone photoreceptors in the retina of the ground squirrel. Vis Neurosci 15:685–691.

Mastrangelo M, Schleich CE, Zenuto RR. 2009. Short-term effects of an acute exposure to predatory cues on the spatial working and reference memory performance in a subterranean rodent. Anim Behav 77:685–692.

Mills SL, Catania KC. 2004. Identification of retinal neurons in a regressive rodent eye (the naked mole rat). Vis Neurosci 21:107–117.

Nemec P, Burda H, Peichl L. 2004. Subcortical visual system of the African mole-rat *Cryptomys anselli*: to see or not to see? Eur J Neurosci 20:757–768.

Nemec P, Cveková P, Burda H, Benada O, Peichl L. 2007. Visual systems and the role of vision in subterranean rodents: diversity of retinal properties and visual system designs. In: Begall S, Burda H, Schleich CE, editors. Subterranean rodents: news from underground. Berlin: Springer. p 129–160.

Nemec P, Cveková P, Benada O, Wielkopolska E, Olkowicz S, Turlejski K, Burda H, Bennett NC, Peichl L. 2008. The

visual system in subterranean African mole-rats (Rodentia, Bathyergidae): retina, subcortical visual nuclei and primary visual cortex. Brain Res Bull 75:356–364.

Nevo E. 2000. Mosaic evolution of subterranean mammals: regression, progression and global convergence. Oxford: Oxford University Press.

Palacios AG, Varela FJ, Srivastava R, Goldsmith TH. 1998. Spectral sensitivity of cones in the goldfish, Carassius auratus. Vis Res 38:2135–2146.

Parry JW, Poopalasundaram S, Bowmaker JK, Hunt DM. 2004. A novel amino acid substitution is responsible for spectral tuning in a rodent violet-sensitive visual pigment. Biochemistry 43:8014–8020.

Peichl L. 2005. Diversity of mammalian photoreceptor properties: Adaptations to habitat and lifestyle? Anat Rec A 287: 1001–1012

Peichl L, Moutairou K. 1998. Absence of short-wavelength sensitive cones in the retinae of seals (Carnivora) and African giant rats (Rodentia). Eur J Neurosci 10:2586–2594.

Peichl L, Künzle H, Vogel P. 2000. Photoreceptor types and distributions in the retinae of insectivores. Vis Neurosci 17:937–948.

Peichl L, Nemec P, Burda H. 2004. Unusual cone and rod properties in subterranean African mole-rats (Rodentia, Bathyergidae). Eur J Neurosci 19:1545–1558.

Peichl L, Chavez AE, Ocampo A, Mena W, Bozinovic F, Palacios AG. 2005. Eye and vision in the subterranean rodent cururo (*Spalacopus cyanus*, Octodontidae). J Comp Neurol 486:197–208.

Rado R, Gev H, Goldman BD, Teruel J. 1991. Light and circadian activity in the blind mole-rat. In: Ricklis E, editor. Photobiology. New York: Plenum Press. p 581–587.

Rado R, Brontchi G, Wollberg Z, Terkel J. 1992. Sensitivity to light of the blind mole-rat. Isr J Zool 38:323–331.

Rocha FA, Ahnelt PK, Peichl L, Saito CA, Silveira LCL, de Lima, SMA. 2009. The topography of cone photoreceptors in the retina of a diurnal rodent the agouti (*Dasyprocta aguti*). Vis Neurosci 26:167–175.

Roessel van P, Palacios AG, Goldsmith TH. 1997. Activity of long-wavelength cones under scotopic conditions in the cyprinid fish *Danio aequipinnatus*. J Comp Physiol A 181: 493–500.

Sanyal S, Jansen HG, DeGrip WJ, Nevo E, de Jong WW. 1990. The eye of the blind mole rat, *Spalax ehrenbergi*. Rudiment with hidden function? Invest Ophthalmol Vis Sci 31: 1398–1404.

Schiviz AN, Ruf T, Kuebber-Heiss A, Schubert C, Ahnelt PK. 2008. Retinal cone topography of artiodactyl mammals: Influence of body height and habitat. J Comp Neurol 507: 1336–1350.

Slobodchikoff CN, Paseka A, Verdolin JL. 2009. Prairie dog alarm calls encode labels about predator colors. Anim Cogn 12:435–439.

Stavenga DG, Smits RP, Hoenders BJ. 1993. Simple exponential functions describing the absorbance bands of visual pigment spectra. Vision Res 33:1011–1017.

Wang Y, Macke JP, Merbs SL, Zack DJ, Klaunberg B, Benett J, Gearhart J, Nathans J. 1992. A locus control region adjacent to the human red and green visual pigment genes. Neuron 9:429–440.

Wegner RE, Begall S, Burda H. 2006: Light perception in 'blind' subterranean Zambian mole-rats. Anim Behav 72: 1021–1024.

Williams GA, Calderone JB, Jacobs GH. 2005. Photoreceptors and photopigments in a subterranean rodent, the pocket gopher (*Thomomys bottae*). J Comp Physiol A 191: 125–134.

Yokoyama S. 2000. Molecular evolution of vertebrate visual pigments. Prog Retin Eye Res 19:385–419.

Yokoyama S, Radlwimmer FB, Kawamura S. 1998. Regeneration of ultraviolet pigments of vertebrates. FEBS Lett 423: 155–158.